

# Quantitative Wavelength-Dependent Photochemistry of the [CpFe( $\eta^6$ -ipb)]PF<sub>6</sub> (ipb = Isopropylbenzene) Photoinitiator

Vladimír Jakúbek and Alistair J. Lees\*

Department of Chemistry, State University of New York at Binghamton,  
Binghamton, New York 13902-6016

Received June 15, 2000

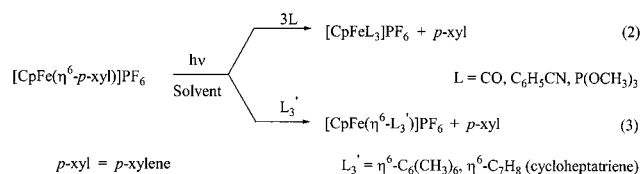
The photochemically induced arene dissociation reaction of the widely used cationic photoinitiator complex [CpFe( $\eta^6$ -isopropylbenzene)]PF<sub>6</sub> has quantitatively been investigated in several different solvents at 293 K as a function of excitation wavelength at 355, 458, 488, 514, 633, and 683 nm. The complex was excited into the lowest-lying singlet ligand field manifold (355–514 nm) and directly into the corresponding lowest-lying triplet ligand field state (633, 683 nm). Absolute photochemical quantum efficiency ( $\phi_{cr}$ ) results reveal that the system exhibits a strong excitation wavelength dependence in each investigated solvent and that the reaction is extremely efficient in the UV and visible regions. The wavelength dependence also reveals that the photochemistry does not occur solely from the lowest-lying ligand field triplet excited state. New insights in terms of both photophysical and mechanistic aspects of this system are obtained from the quantitative photochemical results.

## Introduction

The photochemistry of cationic iron sandwich complexes of the general formula [CpFe( $\eta^6$ -arene)]X (Cp =  $\eta^5$ -C<sub>5</sub>H<sub>5</sub>; X = counterion) has been the focus of many research efforts since the initial discovery of photodecomposition by Nesmeyanov et al.:<sup>1</sup>



Detailed research studies have revealed that these 18-electron Fe<sup>II</sup> (d<sup>6</sup>) sandwich complexes possess interesting photochemical and photophysical properties.<sup>1–12</sup> Concerning the photochemistry, it is significant that Gill and Mann have reported the formation of CpFeL<sub>3</sub> in the presence of a suitable two-electron donor ligand L (L = CO, C<sub>6</sub>H<sub>5</sub>CN, P(OCH<sub>3</sub>)<sub>3</sub>) (eq 2) and arene replacement in the presence of a six-electron donor ligand L<sub>3</sub>' (L<sub>3</sub>' = C<sub>6</sub>(CH<sub>3</sub>)<sub>6</sub>, C<sub>7</sub>H<sub>8</sub>) (eq 3) following irradiation of the [CpFe( $\eta^6$ -arene)]X system.<sup>3,4</sup>

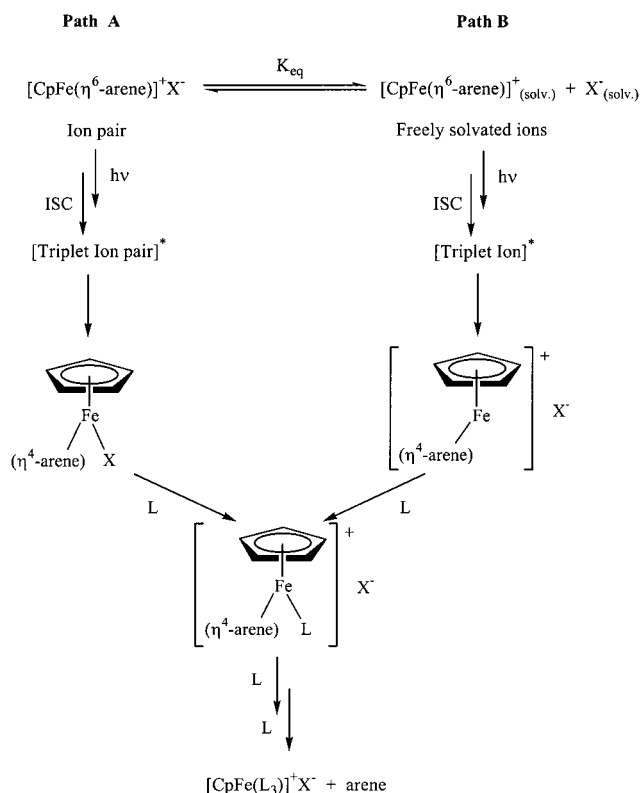


In a comprehensive series of studies carried out at 436 nm, the quantum efficiency of arene loss was measured and found to be dependent on changes in the substituent groups on the Cp ligand, the nature of the arene, the polarity of the solvent, and the nucleophilicity of the counterion (X).<sup>5</sup> Moreover, quantitative triplet sensitization and studies at longer excitation wavelength have revealed that the lowest-lying ligand field triplet state is responsible for this reaction.<sup>5–9,12</sup>

An interpretation of the solvent dependence in the terms of a mechanism involving ion-paired and freely solvated species has been provided by Schuster et al. (Scheme 1).<sup>10</sup> In solvents with a low dielectric constant the complex exists predominantly as the ion pair [CpFe( $\eta^6$ -arene)]<sup>+</sup>X<sup>-</sup>, which upon irradiation forms a neutral ring slipped  $\eta^4$ -arene intermediate containing a coordinated counterion. Subsequently, a molecule of L (two-electron donor ligand) replaces the counterion (X) in the  $\eta^4$ -arene intermediate via a much slower thermal step to yield [CpFe( $\eta^4$ -arene)L]<sup>+</sup> (path A). However, in solvents with a high dielectric constant the dissociation of the ion pair into freely solvated ions is preferred. Here, upon irradiation, the cationic coordinatively unsaturated ring slipped  $\eta^4$ -arene intermediate is formed, and this reacts rapidly and thermally with a molecule of L to produce [CpFe( $\eta^4$ -arene)L]<sup>+</sup> (path B). Thereafter, these two pathways converge and two molecules of L displace the partially bound and slipped  $\eta^4$ -arene, in two subsequent thermal steps, to produce the trisubstituted product [CpFeL<sub>3</sub>]<sup>+</sup>. It should be noted that 532 nm irradiation into the lowest-lying singlet states of either the ion pair or the freely solvated ion and sensitization experiments that bypass these singlet states were observed to result in the same reaction intermediates. This

- (1) Nesmeyanov, A. N.; Volkenau, N. A.; Shilovtseva, L. S. *Dokl. Akad. Nauk SSSR* **1970**, *190*, 857.
- (2) Geoffroy, G. L.; Wrighton, M. S. *Organometallic Photochemistry*; Academic Press: New York, 1979.
- (3) Gill, T. P.; Mann, K. R. *Inorg. Chem.* **1980**, *19*, 3007.
- (4) Gill, T. P.; Mann, K. R. *J. Organomet. Chem.* **1981**, *216*, 65.
- (5) Schrenk, J. L.; Palazzotto, M. C.; Mann, K. R. *Inorg. Chem.* **1983**, *22*, 4047.
- (6) Gill, T. P.; Mann, K. R. *Organometallics* **1982**, *1*, 485.
- (7) Gill, T. P.; Mann, K. R. *Inorg. Chem.* **1983**, *22*, 1986.
- (8) McNair, A. M.; Schrenk, J. L.; Mann, K. R. *Inorg. Chem.* **1984**, *23*, 2633.
- (9) Schrenk, J. L.; Mann, K. R. *Inorg. Chem.* **1986**, *25*, 1906.
- (10) Chrisope, D. R.; Park, K. M.; Schuster, G. B. *J. Am. Chem. Soc.* **1989**, *111*, 6195.
- (11) Roman, E.; Barrera, M.; Hernandez, S.; Lissi, E. *J. Chem. Soc., Perkin Trans. 2* **1988**, 939.
- (12) Mann, K. R.; Blough, A. M.; Schrenk, J. L.; Koefod, R. S.; Freedman, D. A.; Matatchek, J. R. *Pure Appl. Chem.* **1995**, *67*, 95 and references therein.

## Scheme 1



observation verified the existence of efficient intersystem crossing (ISC) from singlets into their corresponding lower-energy triplets and confirmed the reactive role for the triplet manifold. However, the reactive participation of the singlet manifold was not excluded for cases where the singlet excited states were populated directly.

Concurrent with the interpretation of the solvent dependence, visible fluorescence at 520 nm following 430 nm excitation was detected by Roman et al. for several  $[\text{CpFe}(\eta^6\text{-arene})]\text{X}$  complexes at room temperature.<sup>11</sup> It was noted that the fluorescence quantum efficiencies ( $\phi_f$ ) of the molecules increased with the number of methyl groups on the arene ligand. Interestingly, the quantum efficiency for fluorescence of  $[\text{CpFe}(\eta^6\text{-}p\text{-xylene})]^+$  was observed to increase with the presence of hexamethylbenzene in solution, and at higher concentration the  $\phi_f$  values almost reached that observed for  $[\text{CpFe}(\eta^6\text{-hexamethylbenzene})]^+$ . This finding led to the proposition that arene exchange occurs on the singlet excited-state surface without significant deactivation of the complex.<sup>11</sup>

Recently, cationic iron sandwich complexes of the general formula  $[\text{CpFe}(\eta^6\text{-arene})]\text{X}$  (arene = benzene, toluene, hexamethylbenzene, naphthalene, anthracene, pyrene; X =  $\text{BF}_4$ ,  $\text{PF}_6$ ,  $\text{SbF}_6$ ,  $\text{AsF}_6$ ,  $\text{CF}_3\text{SO}_3$ ) have been shown to be effective cationic photoinitiators in the polymerization of epoxides,<sup>13–15</sup> dicyanate esters,<sup>16–18</sup> pyrrole,<sup>19,20</sup> styrene,<sup>21</sup> dioxolones,<sup>22</sup> and acry-

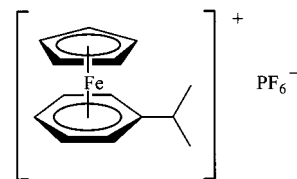


**Figure 1.** Structure of the 18-electron ( $d^6$ )  $[\text{CpFe}(\eta^6\text{-ipb})]\text{PF}_6$  complex.

lates.<sup>21,23,24</sup> Consequently, complexes such as  $[\text{CpFe}(\eta^6\text{-ipb})]\text{PF}_6$  (ipb = isopropylbenzene) (Figure 1) are used widely in industrial polymerization processes, including the manufacture of printed circuit boards,<sup>25–29</sup> microlithography,<sup>30</sup> and other coating applications.<sup>31</sup>

Despite the importance of these cationic iron sandwich complexes, our knowledge of the quantitative photochemistry of  $[\text{CpFe}(\eta^6\text{-arene})]\text{X}$  is very limited. All quantitative investigations to date have only employed excitations at 436 nm to avoid the light absorption that takes place by the entering ligand at higher energy and the low absorptivity of complexes at lower energy. At this wavelength the lowest-lying ligand field (LF) absorption manifold is populated, and it has been assumed that the quantum efficiency for intersystem crossing is unity and that the reactivity occurs exclusively from a lowest-energy LF triplet state ( $a^3E_1$ ).<sup>8</sup> However, we have recently developed a photokinetic procedure that enables one to study in detail the wavelength dependence of the photoreactivity in systems where there are substantial inner filter absorbances.<sup>32</sup> Here, we report full details of the first quantitative wavelength dependence investigation of the  $[\text{CpFe}(\eta^6\text{-arene})]\text{X}$  complex, following our earlier communication.<sup>33</sup> Quantitative results have been obtained for  $[\text{CpFe}(\eta^6\text{-ipb})]\text{PF}_6$  in various solvents over a wide range of excitation wavelengths, and they clearly show that the photochemistry does not occur solely from the lowest-energy triplet excited LF state and that the corresponding singlet state also participates directly in the reactivity.

## Experimental Section

**Materials.** Cyclopentadienyl(isopropylbenzene)iron(II) hexafluorophosphate, tris(1,10-phenanthroline)iron(II) bis(hexafluorophosphate), and phen (1,10-phenanthroline) were purchased from Aldrich Chemical Co. in high purity and used as received. Solvents used in the photoreactivity measurements were purchased from Fisher Scientific Co. and Aldrich Chemical Co. as spectroscopic or HPLC grades. Nitrogen gas used for solvent deoxygenation was purchased as high research grade (Union Carbide, >99.99% purity) and was itself deoxygenated and dried by passage over calcium sulfate (W. A.

(13) Meier, K.; Zweifl, H. *J. Imaging Sci.* **1986**, *30*, 174.

(14) Roloff, A.; Meier, K.; Reideker, M. *Pure Appl. Chem.* **1986**, *58*, 1267.

(15) Park, K. M.; Schuster, G. B. *J. Organomet. Chem.* **1991**, *402*, 355.

(16) McCormick, F. B.; Brown-Wensley, K. A.; DeVoe, R. *J. Polym. Mater. Sci. Eng.* **1992**, *66*, 460.

(17) Kotch, T. G.; Lees, A. J.; Fuerniss, S. J.; Papatomas, K. I.; Snyder, R. *Polym. Mater. Sci. Eng.* **1992**, *66*, 462.

(18) Kotch, T. G.; Lees, A. J.; Fuerniss, S. J.; Papatomas, K. I. *Chem. Mater.* **1995**, *7*, 801.

(19) Rabek, J. F.; Lucki, J.; Zuber, M.; Qu, B. J.; Shi, W. F. *Polymer* **1992**, *33*, 4838.

(20) Rabek, J. F.; Lucki, J.; Zuber, M.; Qu, B. J.; Shi, W. F. *J. Macromol. Sci. Pure Appl. Chem.* **1992**, *A29*, 297.

(21) Wang, P.; Shen, Y.; Wu, S.; Adamczak, E.; Linden, L.; Rabek, J. F. *J. Macromol. Sci. Pure Appl. Chem.* **1995**, *A32*, 1973.

(22) Bolln, C.; Frey, H.; Muelhaupt, R. *J. Polym. Sci., Part A: Polym. Chem.* **1995**, *33*, 587.

(23) Eisele, G.; Fouassier, J. P.; Reeb, R. *Angew. Makromol. Chem.* **1996**, *239*, 169.

(24) Allen, N. S.; Edge, M.; Jasso, A. R.; Corrales, T.; Tellez-Rosas, M. *J. Photochem. Photobiol., A* **1997**, *102*, 253.

(25) Reiser, A. *Photoreactive Polymers: The Science and Technology of Resists*; Wiley-Interscience: New York, 1989.

(26) Kutal, C.; Willson, C. G. *Inf. Rec. Mater.* **1989**, *17*, 373.

(27) Rubner, R. *Adv. Mater.* **1990**, *2*, 452.

(28) Thompson, L. F.; Willson, C. G.; Tagawa, S. *Polymers for Microelectronics. ACS Symp. Ser.* **1994**, 537.

(29) Bühler, N.; Belluš, D. *Pure Appl. Chem.* **1995**, *67*, 25.

(30) Thompson, L. F.; Willson, C. G.; Bowden, M. J., Eds. *Introduction to Microlithography*, 2nd ed.; American Chemical Society: Washington, DC, 1994.

(31) Pietschmann, N.; Schulz, H. *Coating* **1996**, *29*, 270.

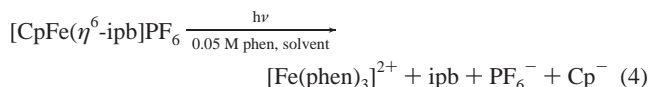
(32) Lees, A. *J. Anal. Chem.* **1996**, *68*, 226.

(33) Jakubek, V.; Lees, A. *J. Chem. Commun.* **1999**, 1631.

Hammond Co.), phosphorus pentoxide (Aldrich Chemical Co.), and a pelletized copper catalyst (BASF R3-11, Chemical Dynamics Co.) that had been activated with hydrogen gas (Union Carbide, >99% purity), according to a previously described procedure.<sup>34</sup>

**Photochemical Procedures.** Photolysis experiments at 355 and 683 nm were performed with a Nd:YAG laser (Molelectron Corp. model MY-34); the latter excitation wavelength was obtained by utilizing a Raman shift of the laser line.<sup>35</sup> Photolyses at 458, 488, and 514 nm were performed with an argon-ion laser (Lexel Corp. model 95-4, 4 W for all lines), and photolysis at 633 nm was performed with a combination of He-Ne lasers (Uniphase model 1105P and Hughes model 3222 H-PC, 13 mW total laser power). Except at 633 nm, a neutral density filter was used to lower the light intensity, and, in all cases, a lens was used to significantly expand the beam to within the size of the photolysis cell; these experimental conditions were applied to avoid any complications associated with two-photon processes and solution inhomogeneity. The incident laser light intensities at all excitation wavelengths were calibrated by means of an Ophir Optonics Ltd. external power meter with a Nova-Display. These light intensities were also verified by ferrioxalate<sup>36–38</sup> and Aberchrome 540 actinometry.<sup>39,40</sup> Typically, the incident light intensities were in the range  $5.8 \times 10^{-7}$  to  $1.0 \times 10^{-6}$  einstein  $\text{min}^{-1}$ . UV-visible absorption spectra recorded during photolysis sequences were obtained on a Hewlett-Packard model 8450A diode-array spectrometer, and the reported band maxima are considered accurate to  $\pm 2$  nm.

During these irradiation experiments, the solution temperatures were controlled to  $\pm 0.1$  K by circulating a thermostated ethylene glycol-water mixture through a jacketed cell holder. Prior to light excitation, the solutions were stringently filtered through 0.22  $\mu\text{m}$  Millipore filters and deoxygenated by purging with prepurified nitrogen gas for 15 min. Typical concentrations in solutions were 1 and 50 mM for [CpFe( $\eta^6$ -ipb)]PF<sub>6</sub> and phen, respectively. Throughout photolysis, the solutions were rapidly stirred to ensure sample homogeneity and uniform absorbance in the light path. The samples were contained in regular 1 cm quartz cuvettes and UV-visible spectra were obtained from solutions at regular time intervals during irradiation. Quantum efficiencies for chemical reaction ( $\phi_{\text{cr}}$ ) to form product,



were obtained by measuring the concentration changes during photolysis over the initial 10–12% of reaction and were corrected for inner filter effects according to a previously described procedure.<sup>32</sup> The systematic errors in the resultant quantum efficiency results are considered to be  $\pm 5\%$  at each excitation wavelength. The [Fe(phen)<sub>3</sub>]<sup>2+</sup> photoproduct was detected spectrophotometrically, and this was confirmed by comparing the spectral bands observed in the photolysis to those observed from a purchased sample of [Fe(phen)<sub>3</sub>]<sup>2+</sup>. It should be noted that in each case the [Fe(phen)<sub>3</sub>]<sup>2+</sup> photoproduct is formed completely and according to the stoichiometry shown in eq 4. This was verified by determining the experimental value of the extinction coefficient of the photoproduct through a photolysis sequence to completion and finding this result to agree (within 5% error) with the known extinction coefficient of the product. Moreover, spectra obtained at any point during the photolysis were not subject to change because of thermal events. These observations demonstrate that the photochemical reaction was uncomplicated by any thermal processes or secondary photoreactions during our irradiations. In the activation energy experiments, the

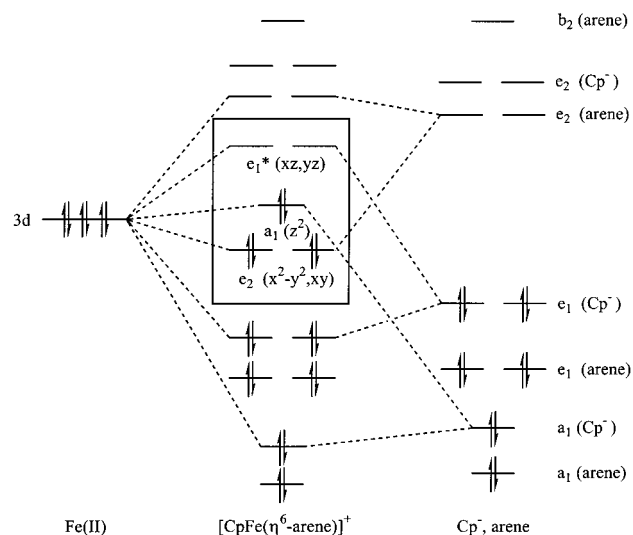


**Figure 2.** Qualitative molecular orbital diagram for [CpFe( $\eta^6$ -benzene)]<sup>+</sup> cation. A box depicts the molecular orbitals that contain appreciable metal d-orbital character.

errors were determined by using standard deviations from individual quantum efficiency measurements.

## Results and Discussion

**Electronic Structure and Spectroscopy.** The electronic structure and spectroscopy of [CpFe( $\eta^6$ -ipb)]PF<sub>6</sub> can be understood by examining the qualitative molecular orbital diagram of the complex [CpFe( $\eta^6$ -benzene)]<sup>+</sup> (Figure 2).<sup>41,42</sup> Clearly, the binding situation in mixed d<sup>6</sup> sandwich systems, such as [CpFe( $\eta^6$ -benzene)]<sup>+</sup>, is essentially similar to that existing in the FeCp<sub>2</sub> and [Fe( $\eta^6$ -benzene)<sub>2</sub>]<sup>2+</sup> systems. Although these complexes formally no longer have the high symmetry of the FeCp<sub>2</sub> ( $D_{5d}$  or  $D_{5h}$ ) and [Fe( $\eta^6$ -benzene)<sub>2</sub>]<sup>2+</sup> ( $D_{6h}$ ) systems, they may still be conveniently treated as having pseudoaxial symmetry, recognizing there is no natural center of inversion (no *u* or *g* distinction).

In idealized cases, the five  $p\pi$  orbitals of the cyclopentadienyl ring and six  $p\pi$  orbitals of the benzene ring form the symmetry-adapted combinations a<sub>1</sub>, e<sub>1</sub>, e<sub>2</sub> and a<sub>1</sub>, e<sub>1</sub>, e<sub>2</sub>, b<sub>2</sub>, respectively. Interaction of these ligand orbitals with the metal 3d valence orbitals of appropriate symmetry generates the molecular orbitals characteristic of the complex. The strongest interaction occurs between the 3d<sub>xz</sub>, 3d<sub>yz</sub> orbitals and the energetically closer Cp ligand e<sub>1</sub> orbitals, rather than the more distant benzene ligand e<sub>1</sub> orbitals. The resulting e<sub>1</sub> molecular orbitals (not marked in Figure 2), formally the highest occupied ligand level, are mainly ligand in character with appreciable metal 3d<sub>xz</sub>, 3d<sub>yz</sub> involvement; these are filled with two pairs of electrons and are strongly bonding. In contrast, the corresponding e<sub>1</sub>\* antibonding orbitals are mostly metal in character and unoccupied; these antibonding orbitals are the lowest unoccupied molecular orbitals in the complex.<sup>42,43</sup> However, it is understood that there also is considerable arene and Cp characters in these e<sub>1</sub>\* antibonding orbitals, as determined for the 19-electron [CpFe( $\eta^6$ -benzene)] complex (17% and 30%, respectively).<sup>46</sup> The weak interaction

(34) Schadt, M. J.; Gresalfi, N. J.; Lees, A. J. *Inorg. Chem.* **1985**, *24*, 2942.

(35) Minck, R. W.; Terhune, R. W.; Rado, W. G. *Appl. Phys. Lett.* **1963**, *3*, 181.

(36) Parker, C. A. *Proc. R. Soc. London, Ser. A* **1953**, *220*, 104.

(37) Hatchard, C. G.; Parker, C. A. *Proc. R. Soc. London, Ser. A* **1956**, *235*, 518.

(38) Calvert, J. G.; Pitts, J. N. *Photochemistry*; Wiley: New York, 1966.

(39) Heller, H. G.; Langan, J. N. *J. Chem. Soc., Perkin Trans.* **1981**, 341.

(40) Kuhn, H.; Braslavsky, S. E.; Schmidt, R. *Pure Appl. Chem.* **1989**, *61*, 187.

(41) Warren, K. D. *Struct. Bonding (Berlin)* **1976**, *27*, 45.

(42) Clack, D. W.; Warren, K. D. *Struct. Bonding (Berlin)* **1980**, *39*, 1.

(43) The degree of metal character of e<sub>1</sub>\* molecular orbitals in CpFe(benzene) (SOMO in 19-electron Fe<sup>I</sup>(d<sup>7</sup>) isostructural complexes) is 63% (experimental determination)<sup>44,45</sup> and 58%, 53%, and 73% determined theoretically from density functional theory calculations,<sup>44</sup> extended Hückel calculations,<sup>46</sup> and SCF-MS-X $\alpha$  calculations,<sup>46</sup> respectively.



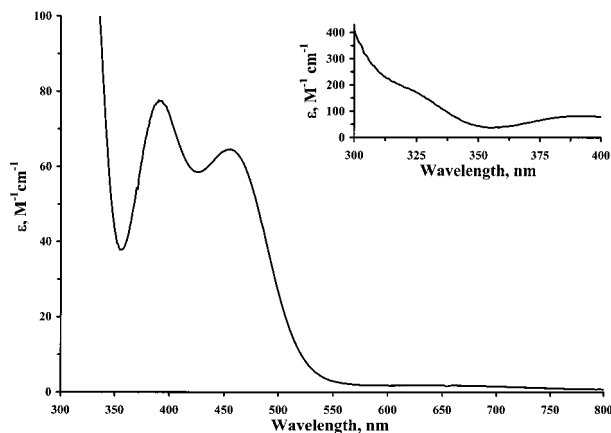


**Figure 3.** UV–visible absorption spectra of  $[\text{CpFe}(\eta^6\text{-ipb})]\text{PF}_6$  in acetone at 293 K. Inset depicts UV absorption spectra in the 300–400 nm region.

between the  $3d_{x^2-y^2}$ ,  $3d_{xy}$  orbitals and the energetically closer benzene ligand  $e_2$  orbitals, rather than the more distant Cp ligand  $e_2$  orbitals, leads to weak bonding, and as consequence, the filled  $e_2$  molecular orbitals retain a large degree ( $\sim 73\%$ ) of metal character.<sup>42</sup> The negligible interaction of the  $3d_{z^2}$  and  $a_1(\text{Cp})$  orbitals results in a nonbonding molecular orbital,  $a_1$ , that is overwhelmingly ( $\sim 94\%$ ) metal in character;<sup>42</sup> this orbital contains two electrons and is the highest occupied molecular orbital in the complex.

Since the  $e_2$ ,  $a_1$ , and  $e_1^*$  molecular orbitals of  $[\text{CpFe}(\eta^6\text{-benzene})]^+$  contain a substantial degree of metal character, the electronic transitions involving these orbitals can be treated within the formalism of ligand field theory.<sup>41,47</sup> The  $^1A_1$  ground state of the  $d^6$  complex corresponds to the  $(e_2)^4(a_1)^2(e_1^*)^0$  electronic configuration. Photoexcitation of an electron in the  $a_1$  orbital to the empty  $e_1^*$  orbitals produces an  $E_1$  excited state, while photoexcitation of an electron in the  $e_2$  orbital to the  $e_1^*$  orbitals results in  $E_2$  and  $E_1$  excited states.

Accordingly, three spin-allowed ligand field transitions are expected to be found in the absorption spectrum of the  $[\text{CpFe}(\eta^6\text{-ipb})]\text{PF}_6$  complex:  $^1A_1 \rightarrow a^1E_1$ ,  $^1A_1 \rightarrow ^1E_2$  and  $^1A_1 \rightarrow b^1E_1$ . Two absorption bands at 458 and 389 nm are observed in the absorption spectrum of  $[\text{CpFe}(\eta^6\text{-ipb})]\text{PF}_6$  in acetone at room temperature (Figure 3). The energy positions of these bands have been determined to be not particularly solvent-dependent, which is typical behavior for  $d-d$  transitions,<sup>2,48–52</sup> and the molar absorptivities of these absorptions are fairly low, consistent with orbitally forbidden transitions in organometallic complexes.<sup>2,48</sup> Consequently, the long-wavelength band at 650 nm with the extremely low absorbance (in acetone,  $\epsilon_{650} = 3.2 \text{ M}^{-1} \text{ cm}^{-1}$ ) is assigned to the spin-forbidden ligand field  $^1A_1 \rightarrow a^3E_1$  transition, in accordance with the previous assignments.<sup>8</sup> The other two spin-forbidden transitions are not resolved within the spectrum. The only solvent-dependent UV absorption band appearing as

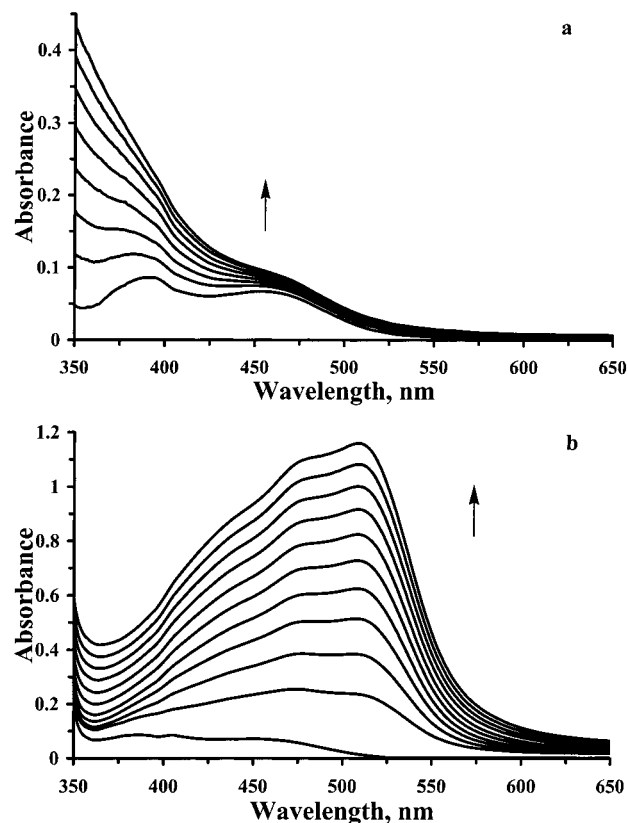


**Figure 4.** UV–visible absorption spectral changes accompanying the 458 nm photolysis of  $1 \times 10^{-3} \text{ M}$   $[\text{CpFe}(\eta^6\text{-ipb})]\text{PF}_6$  in deoxygenated acetone at 293 K: (a) no added phen ligand; (b) containing 0.05 M phen. Spectra are at (a) 3 min and (b) 1 min time intervals. Initial spectra in each case were recorded prior to irradiation.

a shoulder at 325 nm is assigned to a  $d-d$  transition, as noted previously,<sup>52</sup> with some contribution from the arene ligand-to-metal charge transfer (LMCT) transition.<sup>45</sup> The highest-intensity UV bands at 241 and 261 nm have been reassigned to be intraligand  $\pi\pi^*$  transitions involving the Cp ligand rather than the arene ligand.<sup>45</sup> These assignments are consistent with the extensively discussed spectra of  $[\text{CpFe}(\eta^6\text{-arene})]\text{X}$ .<sup>12,45,52</sup>

**Photochemical Reactivity.** The photochemical reactivity of these 18-electron ( $d^6$ )  $[\text{CpFe}(\eta^6\text{-arene})]\text{X}$  complexes, upon irradiation in the 355–683 nm region, is consequently expected to arise from population of the  $e_1^*(d_{xz}, d_{yz})$  orbitals and from depopulation of the  $a_1(d_{z^2})$  and/or  $e_2^*(d_{x^2-y^2}, d_{xy})$  orbitals, which are close-lying. Population of the  $e_1^*(d_{xz}, d_{yz})$  orbitals considerably weakens and lengthens the strong ( $92\text{--}209 \text{ kJ mol}^{-1}$ ) Fe–arene bond.<sup>8</sup> This is consistent with X-ray structural data and the reactivity of  $d^7$   $\text{CpFe}(\text{arene})$  complexes.<sup>46,53,54</sup> In contrast, depopulation of the  $a_1(d_{z^2})$  orbital generates a “hole” in the equatorial belt between the Cp and arene ligands that allows nucleophilic attack of the complex; this is in accordance with X-ray structural data and the known reactivity of  $d^5$   $\text{FeCp}_2^+$  and  $\text{RuCp}_2^+$  complexes.<sup>12</sup>

Photochemical excitation of  $[\text{CpFe}(\eta^6\text{-ipb})]\text{PF}_6$  at 458 nm was performed in various deoxygenated solutions at 293 K. Figure 4a depicts the UV–visible absorption spectra observed accompanying the 458 nm photolysis of the parent complex in acetone at room temperature. During the reaction the intensity

(44) Braden, D. A.; Tyler, D. R. *Organometallics* **2000**, *19*, 1175.

(45) Hamon, J.; Astruc, D.; Michaud, P. *J. Am. Chem. Soc.* **1981**, *103*, 758.

(46) Lacoste, M.; Rabaa, H.; Astruc, D.; Le Beuze, A.; Saillard, J. Y.; Precigoux, G.; Courseille, C.; Ardoin, N.; Bowyer, W. *Organometallics* **1989**, *8*, 2233.

(47) Sohn, Y. S.; Hendrickson, D. N.; Gray, H. B. *J. Am. Chem. Soc.* **1971**, *93*, 3603.

(48) Lees, A. J. *Chem. Rev.* **1987**, *87*, 711.

(49) Manuta, D. M.; Lees, A. J. *Inorg. Chem.* **1983**, *22*, 3825.

(50) Manuta, D. M.; Lees, A. J. *Inorg. Chem.* **1986**, *25*, 3212.

(51) Zulu, M. M.; Lees, A. J. *Inorg. Chem.* **1988**, *27*, 3325.

(52) Morrison, W. H.; Ho, E. Y.; Hendrickson, D. N. *Inorg. Chem.* **1975**, *14*, 500.

(53) Astruc, D.; Hamon, J. R.; Althoff, G.; Roman, E.; Batail, P.; Michaud, P.; Mariot, J. P.; Varret, F.; Cozak, D. *J. Am. Chem. Soc.* **1979**, *101*, 5445.

(54) Hamon, J. R.; Saillard, J. Y.; Le Beuze, A.; McGlinchey, M.; Astruc, D. *J. Am. Chem. Soc.* **1982**, *104*, 7549.

**Table 1.** Absolute Photochemical Quantum Efficiencies ( $\phi_{cr}$ ) for the Arene Dissociation Reaction of [CpFe( $\eta^6$ -ipb)]PF<sub>6</sub> in Various Solvents Following Excitation at Several Wavelengths<sup>a</sup>

solvent	$\phi_{cr}$					
	355 nm	458 nm	488 nm	514 nm	633 nm	683 nm
dichloromethane	0.33(0.02)	0.25(0.001)	0.29(0.003)	0.20(0.003)		0.066(0.002)
acetonitrile	0.66(0.07)	0.64(0.01)	0.62(0.01)	0.49(0.007)	0.20(0.01)	0.15(0.002)
acetone	0.61(0.03)	0.66(0.01)	0.65(0.01)	0.49(0.008)		0.14(0.004)
nitromethane	<i>b</i>	0.72(0.01)	0.72(0.006)	0.55(0.003)		0.17(0.002)
1,2-dichloroethane	0.25(0.02)	0.21(0.001)	0.22(0.002)	0.17(0.002)		0.051(0.002)

<sup>a</sup> Values in parentheses represent the standard deviations from at least five measurements. Phen concentration is 0.05 M in each case. <sup>b</sup> Value was not obtained because of solvent absorption.

of the absorption spectrum increases in the 350–550 nm region; however, no specific absorption band is observed that can be attributed to the photoproducts. This photochemical reaction is further complicated by the formation of precipitate in the solution, as previously described by Nesmeyanov et al.<sup>1</sup> Further investigations in acetone revealed that the precipitate appeared following irradiation in the 458–514 nm region. Under these conditions, where the precipitate complicates the spectral sequence, we were unable to obtain any quantitative data for this photochemical reaction. Similar results were observed for photochemical decomposition of the parent complex following 458 nm irradiation in acetonitrile, nitromethane, methanol, ethanol, and ethylene glycol.

To obtain a clean photochemical reaction for [CpFe( $\eta^6$ -ipb)]PF<sub>6</sub>, the scavenging phen ligand was employed in the reaction system. Figure 4b illustrates UV–visible absorption spectra that have been recorded during the 458 nm photolysis of [CpFe( $\eta^6$ -ipb)]PF<sub>6</sub> in deoxygenated acetone solution containing an excess concentration (0.05 M) of scavenging ligand. The spectral sequence depicted in Figure 4b is representative of those obtained at any of the excitation wavelengths studied and in each case the reaction involves an exceptionally clean conversion to the [Fe(phen)<sub>3</sub>]<sup>2+</sup> photoproduct ( $\lambda_{max}$  = 510 nm), according to eq 4,<sup>8</sup> and was uncomplicated by any thermal processes or secondary photoreactions. When phen is present in excess concentration, it is recognized to act solely as a scavenging ligand and to not affect the reaction kinetics.<sup>5</sup>

**Quantum Efficiencies.** Absolute photochemical quantum efficiencies ( $\phi_{cr}$ ) have been obtained for the arene dissociation reaction of [CpFe( $\eta^6$ -ipb)]PF<sub>6</sub> following excitation in the 355–683 nm region. In each case, the Cp and arene (ipb) ligands were kept the same, and the identical counterion (PF<sub>6</sub><sup>-</sup>) was used in order to eliminate the known effects of these moieties on the  $\phi_{cr}$  values;<sup>5,12</sup> maintaining these factors constant has enabled us to fairly determine excitation wavelength effects. The  $\phi_{cr}$  values were measured according to our previously published procedure, which accounts for inner filter effect absorbances due to the entering ligand and the photoproduct.<sup>32</sup> Such a procedure is much more accurate than the method used earlier (in which  $\phi_{cr}$  values were obtained over a small percentage of reaction to avoid significant photoproduct absorption<sup>3</sup>), and it has also facilitated measurement of  $\phi_{cr}$  data over a wide range of excitation wavelengths, where there are overlapping ligand absorbances or the absorbance from the complex is very low. According to this previously reported photokinetic procedure,<sup>32</sup> the data are predicted to be linear in plots of  $\ln[(A_t - A_\infty)/(A_0 - A_\infty)]$  versus  $\int_0^t [(1 - 10^{-A_{tot}})/A_{tot}] dt$ , where  $A_0$ ,  $A_t$ , and  $A_\infty$  are the absorbance values of the photoproduct at 510 nm during the irradiation and  $A_{tot}$  is the total absorbance at various irradiation times  $t$ . Deviations from linearity are indicative of secondary photochemical or thermal events. However, linearity was indeed observed at each of the excitation wavelengths, and it confirms that there is only one

light step in the photochemistry and no involvement of secondary photoprocesses.

The determined absolute photochemical quantum efficiencies for the arene dissociation reaction of [CpFe( $\eta^6$ -ipb)]PF<sub>6</sub> in various solvents are shown in Table 1. Significantly, the results exhibit a strong wavelength and solvent dependence. In each case, the phen concentration was kept constant and in excess (0.05 M) in order to make a fair comparison across all of the excitation wavelengths. The absolute photochemical quantum efficiencies for the arene dissociation reaction of [CpFe( $\eta^6$ -ipb)]PF<sub>6</sub> in acetonitrile were also determined at various temperatures. Following photolysis at 633 nm directly into the lowest-lying triplet ligand field absorption band, the obtained  $\phi_{cr}$  values are 0.19 (283 K), 0.20 (293 K), 0.21 (303 K), and 0.22 (313 K). The least-squares line of an Arrhenius-type plot of  $\ln \phi_{cr}$  versus  $1/T$  yields an apparent activation energy,  $E_a$ , of  $3.6 \pm 0.5$  kJ mol<sup>-1</sup>. Previously carried out studies of the similar compound [CpFe( $\eta^6$ -*p*-xylene)]BF<sub>4</sub> in acetonitrile following excitation at 436 nm into the lowest-lying singlet ligand field absorption manifold have resulted in  $\phi_{cr}$  values of 0.56 (233 K), 0.62 (253 K), 0.68 (273 K), and 0.71 (293 K) being reported.<sup>8</sup> We have constituted a corresponding Arrhenius-type plot of these earlier data, and this yields an apparent activation energy,  $E_a$ , of  $2.3 \pm 1.2$  kJ mol<sup>-1</sup>.

**Excited-State Reactivity.** Time-resolved absorption spectra obtained for this system by Schuster et al. have also indicated that the initial photochemistry is extremely rapid (on a femto-second or a picosecond time scale) with a dissociative mechanism ( $\eta^6 \rightarrow \eta^4$  arene ring slippage) taking place after initial light absorbance, that the lifetime of the triplet excited state is shorter than 1.5 ns, and that subsequent arene release and ligand scavenging are much slower dark processes ( $k_{bimol} \approx 10^5$ – $10^8$  M<sup>-1</sup> s<sup>-1</sup>).<sup>10,15</sup> It is noteworthy that this sequence of steps and time scales of events is concordant with the ultrafast dynamics observed following UV irradiation of other organometallic compounds undergoing intermolecular C–H/Si–H activation or ligand substitution processes, such as Tp<sup>\*</sup>Rh(CO)<sub>2</sub> (Tp<sup>\*</sup> = HBPz<sub>3</sub><sup>\*</sup>, Pz<sup>\*</sup> = 3,5-dimethylpyrazolyl),<sup>55,56</sup> CpM(CO)<sub>3</sub> (M = Mn, Re),<sup>55,57,58</sup> CpV(CO)<sub>4</sub>,<sup>59</sup> M(CO)<sub>6</sub> (M = Cr, Mo, W),<sup>60,61</sup> and Cr(CO)<sub>4</sub>(bpy) (bpy = 2,2'-bipyridine).<sup>62</sup> In each case, CO

- (55) Yang, H.; Kotz, K. T.; Asplund, M. C.; Wilkens, M. J.; Harris, C. B. *Acc. Chem. Res.* **1999**, *32*, 551.  
 (56) Bromberg, S. E.; Yang, H.; Asplund, M. C.; Lian, T.; McNamara, B. K.; Kotz, K. T.; Yeston, J. S.; Wilkens, M. J.; Frei, H.; Bergman, R. G.; Harris, C. B. *Science* **1997**, *278*, 260.  
 (57) Yang, H.; Kotz, K. T.; Asplund, M. C.; Harris, C. B. *J. Am. Chem. Soc.* **1997**, *119*, 9564.  
 (58) Yang, H.; Asplund, M. C.; Kotz, K. T.; Wilkens, M. J.; Frei, H.; Harris, C. B. *J. Am. Chem. Soc.* **1998**, *120*, 10154.  
 (59) Snee, P. T.; Yang, H.; Kotz, K. T.; Payne, C. K.; Harris, C. B. *J. Phys. Chem. A* **1999**, *103*, 10426.  
 (60) Kotz, K. T.; Yang, H.; Snee, P. T.; Payne, C. K.; Harris, C. B. *J. Organomet. Chem.* **2000**, *596*, 183.  
 (61) Lian, T. Q.; Bromberg, S. E.; Asplund, M. C.; Yang, H.; Harris, C. B. *J. Phys. Chem.* **1996**, *100*, 11994.

dissociation is recognized to take place in less than a few hundred femtoseconds to form a vibrationally hot, coordinatively unsaturated 16-electron complex.<sup>55–64</sup> Indeed, for  $\text{Tp}^*\text{Rh}(\text{CO})_2$  this process has recently been established to occur within 100 fs<sup>63,64</sup> and for the  $\text{M}(\text{CO})_6$  complexes it is recognized to take place within 400 fs.<sup>61,63,64</sup> Subsequently, these unsaturated complexes are solvated in a barrierless reaction and are then vibrationally cooled within a few picoseconds.<sup>55–62</sup> In the case of  $\text{Cr}(\text{CO})_4(\text{bpy})$ , the product of solvation has been determined spectroscopically to be completely formed within 600 fs,<sup>62</sup> and in all the other cases the solvated intermediates have been detected within a few picoseconds after excitation.<sup>55–61</sup> Thereafter, slower thermal processes take place, such as solvent rearrangement and/or solvent substitution, which lead to the final products on picosecond,<sup>59</sup> nanosecond,<sup>55–58</sup> microsecond,<sup>10,58</sup> or millisecond<sup>10</sup> time scales, depending on the specific system.

Consequently, our quantum efficiency data must be rationalized in the context of these ultrafast processes. Clearly, the  $\phi_{\text{cr}}$  results reveal strong dependence on the excitation wavelength for each solvent studied. The arene dissociation reaction clearly proceeds very efficiently following excitation in the 355–514 nm region, which populates the lowest-lying LF singlet manifold, whereas the efficiency of this process is considerably reduced (approximately to 20–30% of the  $\phi_{\text{cr}}$  values obtained for direct singlet irradiation) upon long-wavelength excitation in the 633–683 nm region, which directly populates the LF triplet state (see Table 1 and Figure 3). The  $\phi_{\text{cr}}$  data are not significantly different from 355 to 488 nm for each of the solvents investigated, although we recognize that there is some contribution from the nearby arene ligand-to-metal charge transfer (LMCT) absorption band upon photolysis at 355 nm. It is noted that the efficiency values are also reduced within the singlet manifold; the magnitude of the  $\phi_{\text{cr}}$  data at 514 nm is only 69–80% of the corresponding results at 458 and 488 nm. At 514 nm, the irradiation is understood to populate nearly exclusively the lowest LF singlet state(s) in the manifold. However, photolysis at 458 or 488 nm is likely to result in partial population of upper LF singlet level(s) in addition to the lowest LF single state(s). Thus, the  $\phi_{\text{cr}}$  data at 514 nm are the best indication of quantitative photochemical reactivity from the lowest-lying LF singlet state in this system.

All quantitative investigations of  $[\text{CpFe}(\eta^6\text{-ipb})]\text{PF}_6$  have, to date, employed 436 nm excitation to populate the lowest-lying ligand field manifold. Previously, it has been stated that the quantum efficiencies for intersystem crossing is unity and that the reactivity occurs exclusively from a lowest-energy ligand field triplet state ( $a^3E_1$ ).<sup>8</sup> However, the participation of the reactive singlet ligand field states via direct irradiation was not excluded in later work.<sup>10</sup> Our observed wavelength dependence of  $\phi_{\text{cr}}$  demonstrates unequivocally that the reaction does not occur solely from the lowest-energy triplet level. If the quantum efficiency for intersystem crossing from the lowest-lying singlet excited state ( $a^1E_1$ ) to the triplet reactive state ( $a^3E_1$ ) were unity,<sup>8</sup> then the determined  $\phi_{\text{cr}}$  values would represent the reactive processes only from the lowest-energy triplet state and they would be completely independent of excitation wavelength. To explain our wavelength-dependent quantitative photochemical results, we introduce two alternative photophysical possibilities.

One possibility is that in the  $[\text{CpFe}(\eta^6\text{-ipb})]\text{PF}_6$  complex the lowest-lying singlet ( $a^1E_1$ ) and triplet ( $a^3E_1$ ) LF states have

distinct photoreactive pathways. Recently, independent photochemical reactive routes occurring from lowest-energy singlet and triplet excited states have been proposed in ligand field reactive excited states of  $\text{W}(\text{CO})_5\text{L}$  (L = pyridine and piperidine)<sup>65,66</sup> and  $\text{W}(\text{CO})_4(\text{en})$  (en = ethylenediamine).<sup>67</sup> Furthermore, the utilization of femtosecond and nanosecond pump–probe spectroscopic methods has facilitated the direct identification of the reactive singlet and triplet ligand field states in  $\text{CpMn}(\text{CO})_3$ <sup>57,58</sup> and  $\text{CpV}(\text{CO})_4$ .<sup>59</sup> However, the underlying reasons for the differences in the reactivities of the singlet and triplet excited states in the various complexes are not yet fully established.

To advance a plausible explanation, it is noted that it has been suggested theoretically that transition metal reaction intermediates as triplets exhibit essentially zero affinity for weakly binding molecules such as alkanes (and presumably noble gases).<sup>68–70</sup> This conclusion has been used to explain the high reactivity of triplet ( $\eta^5\text{-Cp}$ )Co(CO) toward  $\text{CpCo}(\text{CO})_2$  in liquefied rare-gas solution or in alkane solution to form a binuclear species.<sup>71</sup> In such instances, the incoming  $\text{CpCo}(\text{CO})_2$  does not require much activation energy to displace an alkane or rare-gas molecule that couples weakly to the metal center of triplet ( $\eta^5\text{-Cp}$ )Co(CO). Furthermore, it has been observed that triplet ( $\eta^5\text{-Cp}$ )Co(CO) reacts with the strongly binding ligand 1-hexene to presumably form a singlet  $\pi$ -complex within picoseconds,<sup>72</sup> while a lifetime on the order of microseconds for triplet ( $\eta^5\text{-Cp}$ )Co(CO) has been found in weakly binding solvents such as Kr and Xe.<sup>71</sup> Hence, the surrounding solvent molecules, especially those interacting strongly with the metal center, need to be considered in describing the reaction coordinate for spin crossover and solvent exchange.

A similar rationale was used to explain the decay of triplet molecules ( $\eta^5\text{-Cp}$ )Mn(CO)<sub>2</sub> and ( $\eta^5\text{-Cp}$ )V(CO)<sub>3</sub> in triethylsilane solutions.<sup>57–59</sup> Thus, it appears that triplet transition metal complexes are preferentially solvated by the more strongly coupling sites of a solvent molecule, which results in thermodynamically more stable products. Subsequently, it has been suggested that the triplet species, which for the most part is long-lived in a nonreactive alkane solvent, is quickly depleted directly via a concerted spin crossover/solvation through the Si–H bond of a solvent  $\text{Et}_3\text{SiH}$  molecule. However, the uncoordinated singlet ( $\eta^5\text{-Cp}$ )Mn(CO)<sub>2</sub> and ( $\eta^5\text{-Cp}$ )V(CO)<sub>3</sub> species are quickly solvated by the ethyl moiety of  $\text{Et}_3\text{SiH}$  to form kinetically solvated products. Considering the above arguments, it is entirely logical to find that in the  $[\text{CpFe}(\eta^6\text{-ipb})]\text{PF}_6$  complex the lowest-lying singlet ( $a^1E_1$ ) and triplet ( $a^3E_1$ ) LF states have distinct photoreactive pathways. The proposed initial reaction mechanism for the arene dissociation reaction for the  $[\text{CpFe}(\eta^6\text{-ipb})]\text{PF}_6$  complex is summarized in Scheme 2 (for purposes of clarity, radiative and nonradiative decay from the excited states and return pathways of reaction intermediates to the parent complex are omitted).<sup>73</sup> The higher

(62) Farrell, I. R.; Matousek, P.; Vlček, A., Jr. *J. Am. Chem. Soc.* **1999**, *121*, 5296.

(63) Joly, A. G.; Nelson, K. A. *Chem. Phys.* **1991**, *152*, 69.

(64) Joly, A. G.; Nelson, K. A. *J. Phys. Chem.* **1989**, *93*, 2876.

(65) Moralejo, C.; Langford, C. H.; Sharma, D. K. *Inorg. Chem.* **1989**, *28*, 2205.

(66) Moralejo, C.; Langford, C. H. *Inorg. Chem.* **1991**, *30*, 567.

(67) Panesar, R. S.; Dunwoody, N.; Lees, A. J. *Inorg. Chem.* **1998**, *37*, 1648.

(68) Blomberg, M. R. A.; Siegbahn, P. E. M.; Svensson, M. *J. Am. Chem. Soc.* **1992**, *114*, 6095.

(69) Siegbahn, P. E. M.; Svensson, M. *J. Am. Chem. Soc.* **1994**, *116*, 10124.

(70) Carroll, J. J.; Weisshaar, J. C.; Haug, K. L.; Blomberg, M. R. A.; Siegbahn, P. E. M.; Svensson, M. *J. Phys. Chem.* **1995**, *99*, 13955.

(71) Bengali, A. A.; Bergman, R. G.; Moore, C. B. *J. Am. Chem. Soc.* **1995**, *117*, 3879.

(72) Dougherty, T. P.; Heilweil, E. J. *J. Chem. Phys.* **1994**, *100*, 4006.

(73) For discussion on precedents for 16-electron organometallics having a triplet ground state see refs 71, 74, and 75.



## Scheme 2

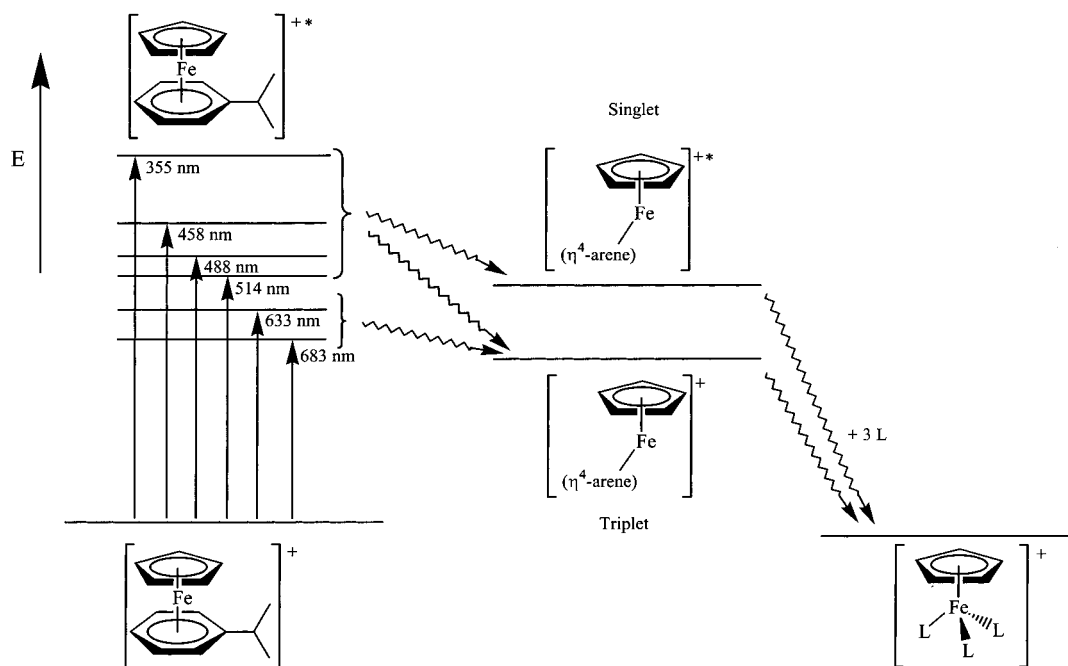


**Table 2.** Ratios of Absolute Photochemical Quantum Efficiencies ( $\phi_{cr(\lambda_{nm})}/\phi_{cr(683nm)}$ ;  $\lambda = 355, 458, 488, 514$  nm) for the Arene Dissociation Reaction of [CpFe( $\eta^6$ -ipb)]PF<sub>6</sub> in Various Solvents<sup>a,b</sup>

solvent	$\phi_{cr(355)}$	$\phi_{cr(458)}$	$\phi_{cr(488)}$	$\phi_{cr(514)}$
	$\phi_{cr(683)}$	$\phi_{cr(683)}$	$\phi_{cr(683)}$	$\phi_{cr(683)}$
acetone	4.4	4.7	4.6	3.5
acetonitrile	4.4	4.3	4.1	3.3
nitromethane	<i>a</i>	4.2	4.2	3.2
1,2-dichloroethane	4.9	4.1	4.3	3.3
dichloromethane	5.0	3.8	4.4	3.0

<sup>a</sup> Quantum efficiency data taken from Table 1. <sup>b</sup> Photolysis at 514 and 683 nm represents excitation into the singlet and triplet absorption bands, respectively.

values of quantum efficiencies are brought about by greater reactivity of the singlet [CpFe( $\eta^4$ -ipb)]<sup>+</sup> species with any interacting part of the solvent molecules, and thus, the rate is dictated by the statistical nature of the solvation process. In contrast, the lower values (within the same solvent) arise because the triplet [CpFe( $\eta^4$ -ipb)]<sup>+</sup> species are less reactive because they bind only to the more strongly coupling sites of the solvent molecules, and the rate is, therefore, determined by thermodynamic considerations as a consequence of preferential solvation.

Significantly, our  $\phi_{cr}$  values lend support to this idea. The different ratios of the absolute photochemical quantum efficiencies for the excitations into the singlet and triplet ligand field manifolds ( $\phi_{cr(355-514\text{ nm})}/\phi_{cr(683\text{ nm})}$ ) and the various solvents are shown in Table 2. As noted above, the  $\phi_{cr}$  data at 514 nm are the best indication of the quantitative photochemical reactivity from the lowest-lying LF singlet state. Hence, the ( $\phi_{cr(514\text{ nm})}/\phi_{cr(683\text{ nm})}$ ) ratio effectively represents the differing singlet and triplet reactivities. These ratios reveal that the greatest change in reactivities between the singlet and triplet states is observed for acetone, where the ratio of the total number of groups to the number of thermodynamically selective groups is the largest.<sup>76</sup> In contrast, the least change in reactivities between singlet and triplet states is observed for dichloromethane, where this ratio is the smallest.<sup>76</sup> Similar trends are noted in the ratios for some of the other singlet manifold

excitation wavelengths, but these data are complicated by the participation of neighboring excited states (vide supra).

Moreover, the possibility of having two distinct photoreactive pathways from the lowest-lying singlet ( $a^1E_1$ ) and triplet ( $a^3E_1$ ) LF states in the [CpFe( $\eta^6$ -ipb)]PF<sub>6</sub> complex may also be interpreted in terms of Hollebone's rules that describe prompt reaction from vibrationally equilibrated LF states.<sup>77-79</sup> This principle has been applied to explain differing singlet and triplet reactivities in other d<sup>6</sup> systems such as W(CO)<sub>5</sub>L (L = pyridine and piperidine)<sup>65,80</sup> and W(CO)<sub>4</sub>(en) (en = ethylenediamine).<sup>67</sup> In these octahedral cases the reduced triplet reactivity has been rationalized in terms of vibronic coupling to a t<sub>1u</sub> asymmetric stretch vibration that does not favor opening a site for nucleophilic attack. On the other hand, the singlet reactivity has been associated with vibronic coupling to a t<sub>1u</sub> buckle mode. Consequently, the increased photoefficiency from the singlet LF state is believed to arise from the fact that in a buckle mode vibration the metal center is exposed to solvating molecules on four octahedral faces.

The second photophysical possibility that we have explored is where the photoreactivity arises exclusively from the singlet level ( $a^1E_1$ ,  $\lambda_{max} = 458$  nm, 261 kJ mol<sup>-1</sup>) and where the long-wavelength photochemistry proceeds via thermal activation from the triplet ( $a^3E_1$ ,  $\lambda_{max} = 650$  nm, 184 kJ mol<sup>-1</sup>) state (a gap of 77.0 kJ mol<sup>-1</sup>). By use of the emission maximum ( $\lambda_{em} = 520$  nm, 230 kJ mol<sup>-1</sup>), observed for other closely related derivatives in this iron system,<sup>11,81</sup> and the absorption maximum of the

(74) Abugideiri, F.; Keogh, D. W.; Poli, R. *J. Chem. Soc., Chem. Commun.* **1994**, 2317.

(75) Detrich, J. L.; Reinaud, O. M.; Rheingold, A. L.; Theopold, K. H. *J. Am. Chem. Soc.* **1995**, *117*, 11745.

(76) The ratios of the total number of groups to the number of thermodynamically selective groups for various solvents are assumed to be (acetone) 3:1, (acetonitrile) 2:1, (nitromethane) 2:1, (1,2-dichloroethane) 4:2, and (dichloromethane) 3:2.

(77) Hollebone, B. R.; Stillman, M. J. *J. Chem. Soc., Faraday Trans. 2* **1978**, 2107.

(78) Hollebone, B. R. *Theor. Chim. Acta* **1980**, *56*, 45.

(79) Hollebone, B. R.; Langford, C. H.; Serpone, N. *Coord. Chem. Rev.* **1981**, *39*, 181.

(80) Langford, C. H.; Moralejo, C.; Lindsay, E.; Sharma, D. K. *Coord. Chem. Rev.* **1991**, *111*, 337.

triplet state, the energy difference between the singlet and triplet ligand field states can be calculated as  $46.0 \text{ kJ mol}^{-1}$ . An estimate of the energy gap from the  $\nu_{0,0}$  transition of the absorption band associated with the triplet ligand field state was impractical because of the very low intensity and the particularly broad character of the absorption band. In the case of the 16-electron  $[\text{CpFe}(\eta^4\text{-ipb})]^+$  complex (Scheme 2), the energy difference between the singlet and triplet states is not assumed to be significantly different from the parent complex. Similarly, for  $(\eta^5\text{-Cp})\text{Mn}(\text{CO})_2$  the energy difference between the singlet and triplet states has been estimated to be 33.8 and 41.3  $\text{kJ mol}^{-1}$ , and for  $(\eta^5\text{-Cp})\text{V}(\text{CO})_3$  it has been estimated as 13.0 and 30.4  $\text{kJ mol}^{-1}$ .<sup>58,59</sup> These values also provide a reasonable assumption of the energy that would be required for a thermal activation process from the triplet excited state to the singlet level. However, the much more substantial difference between the estimated energy gap for the singlet and triplet states ( $46.0 \text{ kJ mol}^{-1}$ ) and our determined apparent activation energy following direct population of the triplet state ( $3.6 \text{ kJ mol}^{-1}$ ) decisively rules out this thermal activation pathway.

Additionally, the  $\phi_{\text{cr}}$  results in Table 1 show a significant solvent dependence for each excitation wavelength, with higher  $\phi_{\text{cr}}$  values being obtained in solvents with high dielectric constants. The lower  $\phi_{\text{cr}}$  values in solvents with low dielectric constants are understood to be caused by ion-pair formation of  $[\text{CpFe}(\eta^6\text{-ipb})]^+\text{PF}_6^-$  and the subsequent participation of the weak nucleophilic counterion in the photochemical mechanism. Previously, time-resolved experiments have indicated that the close interaction of the counterion results in a separate pathway involving a longer-lived ring-slipped ( $\eta^4\text{-arene}$ ) reaction intermediate.<sup>10,12</sup> Such long-lived intermediates incorporating the counterion give additional opportunity for the arene ligand to undergo a reverse ring slippage ( $\eta^4 \rightarrow \eta^6$ ), thereby lowering the  $\phi_{\text{cr}}$  values. The quantum efficiencies, therefore, appear to be reduced by the involvement of the counterion (Scheme 1, path A) rather than direct scavenging by the solvent molecule. Currently, the effects of different solvents on the photochemical mechanism in these complexes are under further investigation.

(81) Although the emission has been assigned to the photoexcited species (ref 11), it is not possible to rule out its arising from one of the rapidly produced reaction intermediates.

In summary, the overall photochemical quantum efficiencies of the arene dissociation from  $[\text{CpFe}(\eta^6\text{-ipb})]\text{PF}_6$  at any excitation wavelength are apparently determined by the branching ratio of the initial ( $\eta^6 \rightarrow \eta^4$ ) dissociative pathway to the nonradiative pathways to the ground state. The photochemical quantum efficiencies are then further diminished by any thermal processes that return the molecule to the initial parent complex, such as a reverse arene ring slippage ( $\eta^4 \rightarrow \eta^6$ ) of the 16-electron  $[\text{CpFe}(\eta^4\text{-ipb})]^+$  complex and any other back-reactions involving counterion and/or solvent rearrangement or substitution.

## Conclusions

This study represents the first one in which the photochemistry of the  $[\text{CpFe}(\eta^6\text{-arene})]\text{X}$  system has been investigated quantitatively at different excitation wavelengths. The results illustrate that the photoreaction is extremely efficient in the UV and visible regions, particularly if polar solvents are employed. Moreover, it is noteworthy that the photochemistry can be effectively performed throughout the visible spectrum, making it possible to use a variety of laser excitation sources; indeed, the triplet state can be populated directly at 683 nm. The wavelength dependence of the photochemistry reveals that the reactivity does not solely derive from the lowest triplet state, as previously assumed.

The strong wavelength dependence in this system may well have a major influence on future photoinitiator applications in coatings, moldings (optical three-dimensional molding), gluing, holography and lithography (laser-stereolithography), and the manufacture of liquid-crystal display devices and protective films for optical devices. Moreover, applications of this photoinitiator may be expanded by the production of new types of polymers with a high level of stereoregularity, by the development of new light-sensitive adhesive sealants, by the food industry, and by the development of new filling multicomponent materials for visible-light-curing in dentistry.<sup>13-31</sup>

**Acknowledgment.** We thank the Division of Chemical Sciences, Office of Basic Energy Sciences, Office of Energy Research, U.S. Department of Energy (Grant DE-FG02-89ER14039) for support of this research. We are also grateful to Shih-Sheng Sun for useful comments.

IC000643F